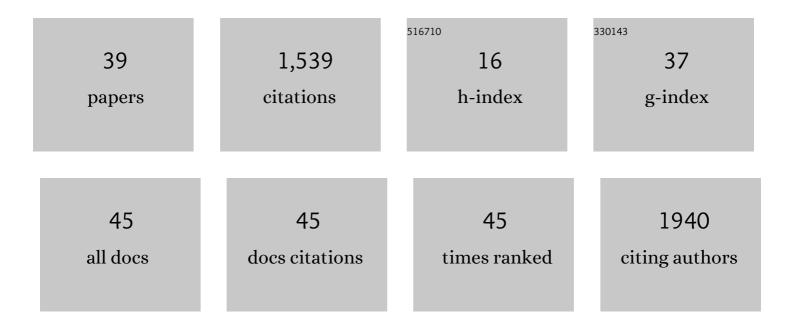
## Marina Piccinelli

List of Publications by Year in descending order

Source: https://exaly.com/author-pdf/7768870/publications.pdf Version: 2024-02-01



#	Article	IF	CITATIONS
1	An image-based modeling framework for patient-specific computational hemodynamics. Medical and Biological Engineering and Computing, 2008, 46, 1097-112.	2.8	621
2	A Framework for Geometric Analysis of Vascular Structures: Application to Cerebral Aneurysms. IEEE Transactions on Medical Imaging, 2009, 28, 1141-1155.	8.9	268
3	High-resolution computational fluid dynamics detects flow instabilities in the carotid siphon: Implications for aneurysm initiation and rupture?. Journal of Biomechanics, 2014, 47, 3210-3216.	2.1	73
4	Low Coronary Wall Shear Stress Is Associated With Severe Endothelial Dysfunction in Patients With Nonobstructive Coronary Artery Disease. JACC: Cardiovascular Interventions, 2018, 11, 2072-2080.	2.9	52
5	Estimation of Inlet Flow Rates for Image-Based Aneurysm CFD Models: Where and How to Begin?. Annals of Biomedical Engineering, 2015, 43, 1422-1431.	2.5	51
6	Automatic Neck Plane Detection and 3D Geometric Characterization of Aneurysmal Sacs. Annals of Biomedical Engineering, 2012, 40, 2188-2211.	2.5	50
7	Coupled Morphological–Hemodynamic Computational Analysis of Type B Aortic Dissection: A Longitudinal Study. Annals of Biomedical Engineering, 2018, 46, 927-939.	2.5	48
8	Geometry of the Internal Carotid Artery and Recurrent Patterns in Location, Orientation, and Rupture Status of Lateral Aneurysms: An Image-Based Computational Study. Neurosurgery, 2011, 68, 1270-1285.	1.1	43
9	3D Fusion of LV Venous Anatomy on Fluoroscopy Venograms With Epicardial Surface on SPECT Myocardial Perfusion Images for Guiding CRT LV Lead Placement. JACC: Cardiovascular Imaging, 2014, 7, 1239-1248.	5.3	43
10	Computed Tomography Evaluation of Autosomal Dominant Polycystic Kidney Disease Progression. Clinical Journal of the American Society of Nephrology: CJASN, 2006, 1, 754-760.	4.5	37
11	An Integrated Statistical Investigation of Internal Carotid Arteries of Patients Affected by Cerebral Aneurysms. Cardiovascular Engineering and Technology, 2012, 3, 26-40.	1.6	31
12	Impact of hemodynamics on lumen boundary displacements in abdominal aortic aneurysms by means of dynamic computed tomography and computational fluid dynamics. Biomechanics and Modeling in Mechanobiology, 2013, 12, 1263-1276.	2.8	23
13	Comprehensive Assessment of Coronary Plaque Progression With Advanced Intravascular Imaging, Physiological Measures, and Wall Shear Stress: A Pilot Doubleâ€Blinded Randomized Controlled Clinical Trial of Nebivolol Versus Atenolol in Nonobstructive Coronary Artery Disease. Journal of the American Heart Association, 2016. 5	3.7	23
14	Advances in Single-Photon Emission Computed Tomography Hardware and Software. Cardiology Clinics, 2016, 34, 1-11.	2.2	19
15	Biomechanical Assessment of Fully Bioresorbable Devices. JACC: Cardiovascular Interventions, 2013, 6, 760-761.	2.9	16
16	Motion Correction and Its Impact on Absolute Myocardial Blood Flow Measures with PET. Current Cardiology Reports, 2018, 20, 34.	2.9	16
17	Diagnostic performance of the quantification of myocardium at risk from MPI SPECT/CTA 2G fusion for detecting obstructive coronary disease: A multicenter trial. Journal of Nuclear Cardiology, 2018, 25, 1376-1386.	2.1	15
18	Novel 3-Dimensional Vessel and Scaffold Reconstruction Methodology for the Assessment of Strut-Level Wall Shear Stress After Deployment of BioresorbableÂVascular Scaffolds From the ABSORB III Imaging Substudy. JACC: Cardiovascular Interventions, 2016, 9, 501-503.	2.9	14

MARINA PICCINELLI

#	Article	IF	CITATIONS
19	Multimodality image fusion for diagnosing coronary artery disease. Journal of Biomedical Research, 2013, 27, 439.	1.6	13
20	Vessel-specific quantification of absolute myocardial blood flow, myocardial flow reserve and relative flow reserve by means of fused dynamic 13NH3 PET and CCTA: Ranges in a low-risk population and abnormality criteria. Journal of Nuclear Cardiology, 2020, 27, 1756-1769.	2.1	11
21	Posttraumatic Stress Disorder, Myocardial Perfusion, and Myocardial Blood Flow: AÂLongitudinal Twin Study. Biological Psychiatry, 2022, 91, 615-625.	1.3	11
22	Advances in Software for Faster Procedure and Lower Radiotracer Dose Myocardial Perfusion Imaging. Progress in Cardiovascular Diseases, 2015, 57, 579-587.	3.1	10
23	Multimodality image fusion, moving forward. Journal of Nuclear Cardiology, 2020, 27, 973-975.	2.1	10
24	Automatic Alignment of Myocardial Perfusion Images With Contrast-Enhanced Cardiac Computed Tomography. IEEE Transactions on Nuclear Science, 2011, 58, 2296-2302.	2.0	7
25	Automatic detection of left and right ventricles from CTA enables efficient alignment of anatomy with myocardial perfusion data. Journal of Nuclear Cardiology, 2014, 21, 96-108.	2.1	6
26	Rationale and design of the quantification of myocardial blood flow using dynamic PET/CTA-fused imagery (DEMYSTIFY) to determine physiological significance of specific coronary lesions. Journal of Nuclear Cardiology, 2020, 27, 1030-1039.	2.1	6
27	Multimodality Image Fusion for Coronary Artery Disease Detection. Annals of Nuclear Cardiology, 2018, 4, 74-78.	0.2	4
28	Dynamic cardiac PET motion correction using 3D normalized gradient fields in patients and phantom simulations. Medical Physics, 2021, 48, 5072-5084.	3.0	3
29	Complete regression of coronary atherosclerosis. European Heart Journal, 2020, 41, 332-332.	2.2	2
30	Integrated 3D Anatomical Model for Automatic Myocardial Segmentation in Cardiac CT Imagery. Lecture Notes in Computational Vision and Biomechanics, 2018, , 1115-1124.	0.5	2
31	Feasibility of Optical Coherence Tomography–Derived Computational Fluid Dynamics in Calcified Vessels to Assess Treatment With Orbital Atherectomy. JACC: Cardiovascular Interventions, 2016, 9, e65-e66.	2.9	1
32	Improved PET-Based Voxel-Resolution Myocardial Blood Flow Analysis. IEEE Transactions on Radiation and Plasma Medical Sciences, 2017, 1, 136-146.	3.7	1
33	Automated and objective removal of bifurcation aneurysms: Incremental improvements, and validation against healthy controls. Journal of Biomechanics, 2019, 96, 109342.	2.1	1
34	Effect of reduced photon count levels and choice of normal data on semi-automated image assessment in cardiac SPECT: Doing more with fewer counts. Journal of Nuclear Cardiology, 2020, 27, 1483-1485.	2.1	1
35	Clinically viable myocardial CCTA segmentation for measuring vessel-specific myocardial blood flow from dynamic PET/CCTA hybrid fusion. European Journal of Hybrid Imaging, 2022, 6, 4.	1.5	1
36	Preparing for the Artificial Intelligence Revolution in Nuclear Cardiology. Nuclear Medicine and Molecular Imaging, 2023, 57, 51-60.	1.0	1

#	ARTICLE	IF	CITATIONS
37	NONINVASIVE VESSEL-SPECIFIC ABSOLUTE MYOCARDIAL BLOOD FLOW AND FLOW RESERVE BY MEANS OF DYNAMIC NH3 PET/CTA IMAGE FUSION: DEVELOPMENT OF NORMAL LIMITS. Journal of the American College of Cardiology, 2016, 67, 1667.	2.8	0
38	Determination of [N-13]-ammonia extraction fraction in patients with coronary artery disease by calibration to invasive coronary and fractional flow reserve. Journal of Nuclear Cardiology, 2022, 29, 2210-2219.	2.1	0
39	Semi-Automatic Reconstruction of Patient-Specific Stented Coronaries based on Data Assimilation and Computer Aided Design. Cardiovascular Engineering and Technology, 2022, , .	1.6	0